



Topical hypochlorous acid (HOCl) blocks inflammatory gene expression and tumorigenic progression in UV-exposed SKH-1 high risk mouse skin

Jana Jandova^{a,b}, Jeremy Snell^{a,b}, Anh Hua^{a,b}, Sally Dickinson^b, Jocelyn Fimbres^{a,b}, Georg T. Wondrak^{a,b,*}

^a Department of Pharmacology and Toxicology, College of Pharmacy and UA Cancer Center, University of Arizona, Tucson, AZ, USA

^b UA Cancer Center, University of Arizona, Tucson, AZ, USA

ARTICLE INFO

Keywords:

Pathway-focused gene expression profiling
Hypochlorous acid
Skin cancer
Solar UV radiation
Inflammation
Oxidative stress

ABSTRACT

Hypochlorous acid (HOCl) is the active oxidizing principle underlying drinking water disinfection, also delivered by numerous skin disinfectants and released by standard swimming pool chemicals used on a global scale, a topic of particular relevance in the context of the ongoing COVID-19 pandemic. However, the cutaneous consequences of human exposure to HOCl remain largely unknown, posing a major public health concern. Here, for the first time, we have profiled the HOCl-induced stress response in reconstructed human epidermis and SKH-1 hairless mouse skin. In addition, we have investigated the molecular consequences of solar simulated ultraviolet (UV) radiation and HOCl combinations, a procedure mimicking co-exposure experienced for example by recreational swimmers exposed to both HOCl (pool disinfectant) and UV (solar radiation). First, gene expression elicited by acute topical HOCl exposure was profiled in organotypic human reconstructed epidermis. Next, co-exposure studies (combining topical HOCl and UV) performed in SKH-1 hairless mouse skin revealed that the HOCl-induced cutaneous stress response blocks redox and inflammatory gene expression elicited by subsequent acute UV exposure (*Nos2*, *Ptgs2*, *Hmox1*, *Srxn1*), a finding consistent with emerging clinical evidence in support of a therapeutic role of topical HOCl formulations for the suppression of inflammatory skin conditions (e.g. atopic dermatitis, psoriasis). Likewise, in AP-1 transgenic SKH-1 luciferase-reporter mice, topical HOCl suppressed UV-induced inflammatory signaling assessed by bioluminescent imaging and gene expression analysis. In the SKH-1 high-risk mouse model of UV-induced human keratinocytic skin cancer, topical HOCl blocked tumorigenic progression and inflammatory gene expression (*Ptgs2*, *Il19*, *Tlr4*), confirmed by immunohistochemical analysis including 3-chloro-tyrosine-epitopes. These data illuminate the molecular consequences of HOCl-exposure in cutaneous organotypic and murine models assessing inflammatory gene expression and modulation of UV-induced carcinogenesis. If translatable to human skin these observations provide novel insights on molecular consequences of chlorination stress relevant to environmental exposure and therapeutic intervention.

1. Introduction

The small molecule electrophile hypochlorous acid (HOCl) is an important endogenous microbicidal component of the innate immune system derived from neutrophil myeloperoxidase (MPO) producing hypohalous acids. However, biological effects, toxicological impact, and potential therapeutic role of HOCl in skin (relevant to environmental toxicant exposure or topical disinfectant use) remain largely unexplored, particularly in the context of HOCl-mediated modulation of inflammatory gene expression and tumorigenesis.

HOCl, in equilibrium with its anionic form [hypochlorite (OCl⁻)] at physiological pH, may also induce tissue damage at sites of inflammation involving the oxidation and chlorination of biomolecules targeting peptides (e.g. glutathione), proteins, lipids, and nucleic acids [1–6]. Dysregulated HOCl production has been shown to contribute to a variety of human pathologies (such as atherosclerosis, rheumatoid arthritis, asthma, neuroinflammation, and cancer) [5–9]. Apart from endogenous HOCl produced in the context of physiological antimicrobial and inflammatory responses, human HOCl exposure can also occur through various exogenous environmental routes [10–14]. Indeed, based on the

* Corresponding author. Department of Pharmacology and Toxicology, College of Pharmacy and UA Cancer Center, University of Arizona, Tucson, AZ, USA.
E-mail address: wondrak@pharmacy.arizona.edu (G.T. Wondrak).

<https://doi.org/10.1016/j.redox.2021.102042>

Received 30 April 2021; Received in revised form 7 June 2021; Accepted 8 June 2021

Available online 11 June 2021

2213-2317/© 2021 The Authors.

Published by Elsevier B.V. This is an open access article under the CC BY-NC-ND license

(<http://creativecommons.org/licenses/by-nc-nd/4.0/>).

use of this powerful and versatile oxidant for freshwater preservation, operative on a global scale for both drinking water supply and public pool sanitation, human skin is subject to environmental HOCl exposure that occurs in the low ppm range [≤ 5 ppm (equating ≤ 100 μM) according to CDC and EPA guidelines] [12,14,15]. Health concerns associated with chlorinated drinking water and recreational exposure during swimming pool attendance have been raised before, particularly with a molecular focus on the role of HOCl and HOCl-derived organic chlorination byproducts. Inhalation, cutaneous exposure, and ingestion of irritant and carcinogenic disinfection byproducts (DBPs) have all been implicated in human pathogenesis (such as respiratory impairment and asthma exacerbation, allergic contact dermatitis, ocular/corneal irritation, and bladder cancer, respectively) [12,16]. Indeed, epidemiological evidence suggests that pool attendance correlates with increased asthma incidence in Olympic swimmers and pool workers, and consequences of HOCl exposure are now recognized as a potential public health concern [10,17–20].

Interestingly, in addition to endogenous and environmental sources, skin HOCl exposure also occurs through application of topical disinfectants employed worldwide as clinical and consumer products, a preventive use with particular relevance to the ongoing COVID-19 pandemic [21–23]. Remarkably, topical HOCl-based therapeutics optimized for sustained release are now serving as FDA-approved drugs for wound management, atopic dermatitis, pruritus, and psoriasis [24,25]. However, in spite of ubiquitous HOCl exposure of human tissues (i.e. cutaneous, pulmonary, and gastrointestinal epithelia), the specific molecular consequences of HOCl-associated electrophilic stress on structure and function of human skin remain largely unexplored.

Solar ultraviolet (UV) radiation is an important component of the skin exposome involved in photodamage and carcinogenesis including NMSC (non-melanoma skin cancer), and potentiation of solar UV-induced cutaneous and systemic injury by co-exposure to other environmental toxicants and pollutants has attracted much attention impacting vulnerable populations worldwide [26–35]. Indeed, toxicants such as heavy metals (e.g. cadmium), metalloids (e.g. arsenic), and organic xenobiotics (e.g. benzopyrenes, dioxin) are established potentiators of solar UV damage [29–35]. HOCl, commonly referred to as ‘swimming pool chlorine’, is the most frequently-used halogen-based oxidizing pool disinfectant, and, according to CDC, there are 10.4 million residential and 309,000 public swimming pools and over 7.3 million hot tubs in the United States alone [11]. However, little prior research has addressed physiological and toxicological impact of HOCl co-exposure with solar UV as it occurs on a global scale in the context of recreational swimming pool use [10,12].

Here, for the first time, in an attempt to define the toxicological impact and potential therapeutic role of skin exposure to topical HOCl, we have profiled HOCl-induced cutaneous stress gene expression examined in reconstructed human epidermis and SKH-1 hairless mouse skin. In addition, using a focused gene array analysis approach, we have investigated the molecular consequences of acute skin HOCl exposure on redox and inflammatory gene expression elicited by subsequent solar simulated ultraviolet (UV) radiation, a procedure mimicking exposure experienced for example by recreational swimmers exposed to both HOCl (pool disinfectant) and UV (solar radiation). Finally, using an established photocarcinogenesis model (UV-exposed SKH-1 high-risk mouse skin) that mimics solar UV-induced carcinogenic initiation followed by tumorigenic progression, a situation relevant to the progression of human actinic keratosis to non-melanoma skin cancer, the effects of topical HOCl administration on inflammatory gene expression and tumorigenesis were examined. Taken together, our data demonstrate that topical HOCl applied at environmentally relevant exposure levels blocks the UV-induced inflammatory gene expression response and suggest feasibility of using topical HOCl formulations for photochemoprevention of solar UV-induced NMSC.

2. Materials and methods

2.1. Chemicals

All chemicals were purchased from Sigma Aldrich (St. Louis, MO, USA).

2.2. Human skin cell culture

Human immortalized keratinocytes (HaCaT) were purchased from ATCC (Manassas, VA, USA) and maintained according to the manufacturer’s instructions. Briefly, keratinocytes were cultured in DMEM medium (Corning, Manassas, VA) supplemented with 10% bovine calf serum (HyClone™ Laboratories, Logan, UT). HOCl exposure was performed in PBS in order to minimize the impact of indirect chlorination reactions (e.g. HOCl-modification of serum proteins in medium that might confound cellular effects). Cells were maintained in a humidified incubator (37 °C, 5% CO₂ and 95% air) [36,37].

2.3. Cell viability analysis by flow cytometry

Cells were treated with HOCl (0–250 μM ; in PBS, 1 h) followed by 23 h post-exposure culture in regular medium. Cell viability was then determined using flow cytometric analysis of annexinV (AV)-propidium iodide (PI) stained cells using an apoptosis detection kit (APO-AF, Sigma, St. Louis, MO) according to the manufacturer’s specifications as published before [38].

2.4. Human epidermal reconstructs

Before treatment, refrigerated epidermal reconstructs (EPI-200™, 9 mm diameter; MatTek, Corp., Ashland, MA) were equilibrated in fresh growth medium (0.9 ml; EPI-200-ASY media per well, 1 h), following our standard procedures for maintenance and treatment as published before [36,38–40]. Briefly, the stratum corneum of air exposed reconstructs was treated with HOCl [100 μM ; in PBS; 30 min or 6 h exposure time, 37 °C; 5% CO₂]. Following exposure, epidermal reconstructs were processed for RNA extraction using the RNeasy Mini kit (Qiagen, Germantown, MD).

Comparative RT² Profiler™ gene expression array analysis: Total mRNA from cultured skin reconstructs or mouse skin was prepared using the RNeasy Mini kit (Qiagen) following our published standard procedures [38,41,42]. Reverse transcription was then performed using the RT² First Strand kit (Qiagen) from a total of 500 ng RNA. Human Oxidative Stress Plus (PAHS-065YA) and mouse Oxidative Stress (PAMM-065ZA) RT² Profiler™ technology (Qiagen) assessing expression of 84 redox regulatory genes was used as published before [42]. Quantitative PCR was run using the following conditions: 95 °C (10 min), followed by 40 cycles at 95 °C (15 s) alternating with 60 °C (1 min) (Applied Biosystems, Carlsbad, CA). Individual genes were normalized to a group of 5 housekeeping genes (human: *ACTB*, *B2M*, *GAPDH*, *HPRT1*, *RPLP0* and mouse: *Actb*, *B2m*, *Gapdh*, *Gusb*, *Hsp90ab1*) and quantified using the comparative $\Delta\Delta\text{Ct}$ method (ABI Prism 7500 sequence detection system user guide).

2.5. Single RT-qPCR analysis

Total RNA from mouse skin was isolated using the Qiagen RNeasy Mini Kit (Qiagen) according to the manufacturer’s protocol. Murine 20X primer/probes [*Nos2* (Mm_00440502_m1), *Ptgs2* (Mm_00478374_m1), *Txnip* (Mm_01265659_g1), *Tlr4* (Mm_00445273_m1), *Iil19* (Mm_01288324_m1), and *Rps18* (Mm_02601777_g1)] were obtained from Fisher Scientific (Waltham, MA). cDNA synthesis was carried out by following cycling conditions using MJ Thermocycler PTC-200 (MJ Research, Watertown, MA): 25 °C for 10 min; 48 °C for 30 min and 95 °C for 5 min and subsequent amplification of target genes by following

conditions using ABI7500 Real-Time PCR System (Applied Biosystems, Foster City, CA): 95 °C for 10 min, 95 °C for 15 s and 60 °C for 1 min for a total of 40 cycles. Amplification of murine housekeeping gene *Rps18* was used to examine the quality of cDNA. Non-template controls were included on each PCR plate. Expression levels of target genes were normalized to *Rps18* control. Amplification plots were generated and the Ct values (cycle number at which fluorescence reaches threshold) recorded as published before [38,42].

2.6. Topical HOCl and UV exposure in the SKH-1 mouse model

For all experiments, six to eight-weeks old female SKH-1 Elite™ mice were purchased from Charles River Laboratories (Wilmington, MA) and housed and maintained in accordance with The University of Arizona Animal Care and Use Committee standards under an approved IACUC protocol (17–298).

2.7. Acute exposure murine model (UV and HOCl)

Mice were randomly allocated to one of the following treatment groups (five mice per group): group 1 (PBS carrier, 30 min, no UV); group 2 (100 μM HOCl, 30 min, no UV); group 3 (PBS carrier, 30 min, UV); group 4 (100 μM HOCl, 30 min, followed by UV). For topical exposure, hydrated gauze covered with Tegaderm™ (3 M Health Care, St. Paul, MN) containing either HOCl or PBS only was placed on the backs of mice (throughout the specified exposure time). Elizabethan collars (Braintree Scientific Inc., Braintree, MA) were used during this pre-treatment phase to avoid scratching-induced interference. Following 30 min pre-treatment, mice (groups 3 and 4) received UV exposure (UVA: 9.2 J/cm²; UVB: 480 mJ/cm²) using a solar simulator source [model 91293 (Oriental Corporation) equipped with a 1000W Xenon arc lamp] as published before [43]. Tissue samples for RNA and IHC were harvested 5h 30 min after topical exposure (6 h total after initiation of experiment).

2.8. Epidermal AP-1 luciferase mouse model

SKH-1 mice expressing [12-O-tetradecanoylphorbol-13-acetate (TPA) response element] (TRE)-driven luciferase responsive to AP-1 transcriptional regulation were available at the UA Cancer Center and bred and maintained as published before [44,45]. Mice were separated into four groups as follows (three mice per group): ‘group 1’ [carrier, Vanicream™ (Pharmaceutical Specialties, Inc. Rochester, MN), no UV], ‘group 2’ (100 μM HOCl in Vanicream™, no UV), ‘group 3’ (Vanicream™, UV), ‘group 4’ (100 μM HOCl in Vanicream™, UV). Vanicream™ (with or without HOCl) was administered twice (dorsal skin; 24 h and 1 h) prior to dorsal UVB exposure (275 mJ/cm²) performed as published recently [44,45]. 24 h post UV exposure, quantitative bioluminescent imaging (Lago, Spectral Instruments Imaging, Tucson, AZ) was performed (using D-luciferin i.p. injection), and skin tissue was harvested for mRNA expression analysis.

2.9. High-risk (tumor-prone) mouse model

To generate the standard UV-exposed SKH-1 ‘high-risk’ (tumor-prone) mouse model, SKH-1 mice were subjected to a UVB exposure regimen as published before [46,47]. An irradiation panel of UVB-313 lamps (Q-LAB, Westlake, OH) was used, and the spectral output was quantified using a dosimeter from International Light Inc. (Newburyport, MA), model IL1700, with an SED240 detector for UVB (range 265–310 nm, peak 285 nm) at a distance of 365 mm from the source. This UV dose regimen delivers 190 mJ/cm² per UV exposure (final dose; three times per week) [first six weeks of UV exposure: increasing dose regimen (week 1–2: 40%; week 3–4: 60%; week 5–6: 80% of final dose per exposure) to allow skin photo-adaptation]. At the end of the 112 d irradiation period, these mice are tumor free but have a high risk for

developing papilloma/squamous cell carcinoma lesions over the next several weeks [46,47]. Two weeks after the end of the UV regimen pair-matched ‘high-risk’ mice (ten mice per group) received either topical HOCl (100 μM in 50 μl Vanicream™) or carrier only (Vanicream™), administered three times per week over a 24 d period, during which tumor development was monitored. At the end of the topical treatment period (38 d after last UV exposure), final tumor volume (cumulative tumor burden per animal) was determined.

2.10. Immunohistochemistry

After collection, tissues were fixed in 10% neutral buffered formalin (NBF) and processed for paraffin embedment. Sections from each tissue block were counterstained with hematoxylin/eosin (H&E) and analyzed for antigen detection: iNOS (NB300-605, Novus Biologicals), IL-19 (PA5-68455, Invitrogen), COX-2 (27308-1-AP, Proteintech), 3-chlorotyrosine epitopes (HP5002, HycultBiotech, Uden, Netherlands), and Ki67 (ab15580, Abcam) following our published procedures [41,42]. In brief, following deparaffinization and hydration, slides were subjected to heated antigen retrieval (citric, pH 6.0 or Tris-EDTA, pH 9.0). After overnight incubation in primary antibody, slides were incubated with biotinylated anti-mouse/anti-rabbit secondary antibody (RTU PK7200, Vector Laboratories, Burlingame, CA, USA) and a subsequent incubation with avidin/biotin streptavidin/horseradish peroxidase (Vectastain ABC, SK-4103, Vector Laboratories). Then, slides were developed with a diaminobenzidine/hydrogen peroxide mixture, counterstained with hematoxylin, dehydrated with graded alcohols and xylene, and mounted using a xylene based medium. Images were captured using an Olympus BX50 and Spot (Model 2.3.0) camera.

2.11. Statistical analysis

Unless stated differently, data sets were analyzed employing analysis of variance (ANOVA) with Tukey’s posthoc test using the GraphPad Prism 9.1.0 software (Prism Software Corp., Irvine, CA); in respective bar graphs (analyzing more than two groups), means without a common letter differ ($p < 0.05$) as published before [42]. For bar graphs comparing two groups only, statistical significance was calculated employing the Student’s two-tailed *t*-test. The level of statistical significance was marked as follows * $p < 0.05$; ** $p < 0.01$; *** $p < 0.001$. Experiments involved at least nine individual replicates per data point, except for gene expression array analysis performed with three independent biological replicates analyzed in triplicate format. Nonparametric data analysis of murine experimentation (average tumor burden) was performed using the Mann–Whitney test. Differences between groups were considered significant at $p < 0.05$.

3. Results

3.1. Array analysis reveals induction of redox stress response gene expression in human reconstructed epidermis (EpiDerm™) exposed to topical HOCl

First, in preparation of our skin reconstruct and murine explorations (Figs. 1–5), we established the dose response relationship of HOCl-induced cytotoxicity in cultured HaCaT human keratinocytes using annexin V-PI flow cytometry (Fig. 1a). To this end, cells were exposed to increasing concentrations of HOCl (up to 250 μM; in PBS, 1 h) followed by 23 h post-exposure culture in regular medium. Using this dose regimen, we observed that HOCl concentrations up to 100 μM were not associated with a significant impairment of viability. Next, human reconstructed epidermis was treated topically (100 μM HOCl in PBS, continuous exposure for 30 min or 6 h; maintained in 6 well format until time of harvest), followed by Oxidative Stress Plus RT² Profiler™ PCR Array analysis (HOCl-exposed relative to PBS control).

Upon prolonged exposure (6 h), five genes (out of a total of 84 genes

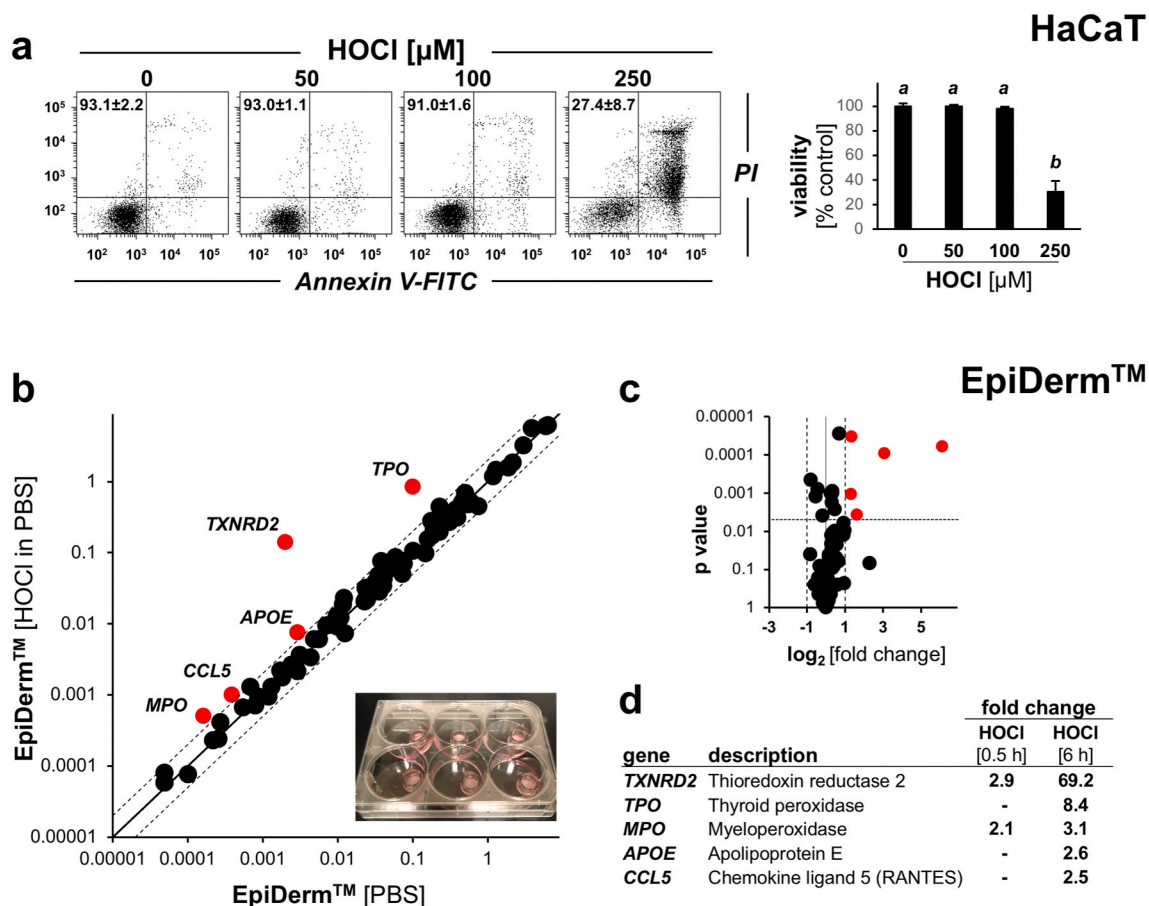


Fig. 1. Array analysis reveals induction of redox stress response gene expression in human reconstructed epidermis (EpiDerm™) exposed to topical HOCl. (a) Dose response relationship of HOCl-induced cytotoxicity (annexin V-PI flow cytometry) in HaCaT keratinocytes exposed to HOCl (0–250 μM ; in PBS, 1 h) followed by postexposure culture (23 h) in regular medium. Panels display representative measurements; numbers in quadrants: percentage of viable cells (AV-negative, PI-negative) from a total of gated cells (mean \pm SD, $n = 3$); bar graph: numerical analysis (normalized to viability of untreated control). (b–d) Human reconstructed epidermis [EpiDerm™; 9 mm diameter in 6 well format; see image insert (panel b)] was treated topically (100 μM HOCl in PBS, 30 min or 6 h, continuous exposure) and cultured until time of harvest, followed by Oxidative Stress Plus RT² Profiler™ PCR Array analysis; scatter (panel b) and volcano (panel c) plots depict differential gene expression [(HOCl-exposed relative to PBS control) cut-off line: expression differential ≥ 2 ; p value < 0.05 ; red dots: upregulated] as presented by tabular summary (panel d). For bar graph depiction, quantitative data analysis employed ANOVA with Tukey's post hoc test; means without a common letter differ from each other ($p < 0.05$). (For interpretation of the references to colour in this figure legend, the reader is referred to the Web version of this article.)

monitored), displayed statistically significant expression changes in response to HOCl treatment as depicted by (i) scatter plot (Fig. 1b), (ii) volcano plot [fold change over p-value (Fig. 1c)], and (iii) tabular summary of statistically significant gene expression changes [fold change ≥ 2 ; p value ≤ 0.05 (Fig. 1d)]. Genes displaying upregulated expression by at least 2-fold (6 h continuous exposure) were identified as *TXNRD2* (encoding mitochondrial thioredoxin reductase 2; 69.2-fold), *TPO* (encoding thyroid peroxidase; 8.4-fold), *MPO* (encoding myeloperoxidase; 3.1-fold), *APOE* (encoding apolipoprotein E; 2.6-fold), and *CCL5* [encoding chemokine C-C motif ligand 5 (RANTES); 2.5-fold]. Remarkably, two of these genes (*TXNRD2*, *MPO*) displayed HOCl-responsiveness with significant upregulation observable even after 30 min exposure only (Fig. 2d). At the same time, MTT-assay based assessment of tissue viability indicated that HOCl treatment (tested at the indicated dose and exposure time range) did not impair epidermal keratinocyte viability (data not shown).

Taken together, these data suggest that short term topical HOCl exposure at environmentally relevant concentrations induces a pronounced skin redox-related gene expression response that involves regulators of mitochondrial redox status (*TXNRD2*), skin barrier function (*APOE*), inflammation (*CCL5*), and reactive halogen species metabolism (*TPO*, *MPO*) [21,48–50].

3.2. Topical HOCl blocks inflammatory gene expression elicited by acute UV exposure in SKH-1 mouse skin

Next, the impact of acute topical HOCl exposure on cutaneous redox and inflammatory gene expression was assessed in SKH-1 mice serving as a relevant *in vivo* model. In addition, this experiment was designed to measure the effect of topical HOCl pre-exposure on subsequent solar UV-induced gene expression (Fig. 2). To this end, mouse skin was pretreated with 'HOCl' [100 μM in carrier (PBS), 30 min; 'groups 2 and 4'] or 'carrier only' ('groups 1 and 3'), followed by 'UV exposure' ('groups 3 and 4') or 'mock UV' treatment ('groups 1 and 2') (Fig. 2a).

First, responsiveness to HOCl treatment ('group 2') was confirmed by gene expression analysis (Oxidative Stress Plus RT² Profiler™ PCR Array) that indicated upregulated expression of redox regulatory genes including *Gss* (encoding glutathione synthetase; 45.8-fold), *Sod3* (superoxide dismutase 3; 2.5-fold), and *Prdx5* (encoding peroxiredoxin 5; 2.1-fold) (Fig. 2b–d). In addition, upregulated expression of NAD(P)H oxidase-related genes including *Ncf2* [encoding neutrophil cytosolic factor 2 (p67/phox); 2.9-fold], *Nox4* (encoding NADPH oxidase 4; 2.3-fold) was observed; likewise, expression of *Noxa1* [encoding NAD(P)H oxidase activator 1; 41.6-fold downregulation] was also responsive to HOCl treatment.

Next, UV-induced gene expression in SKH-1 mouse skin was profiled

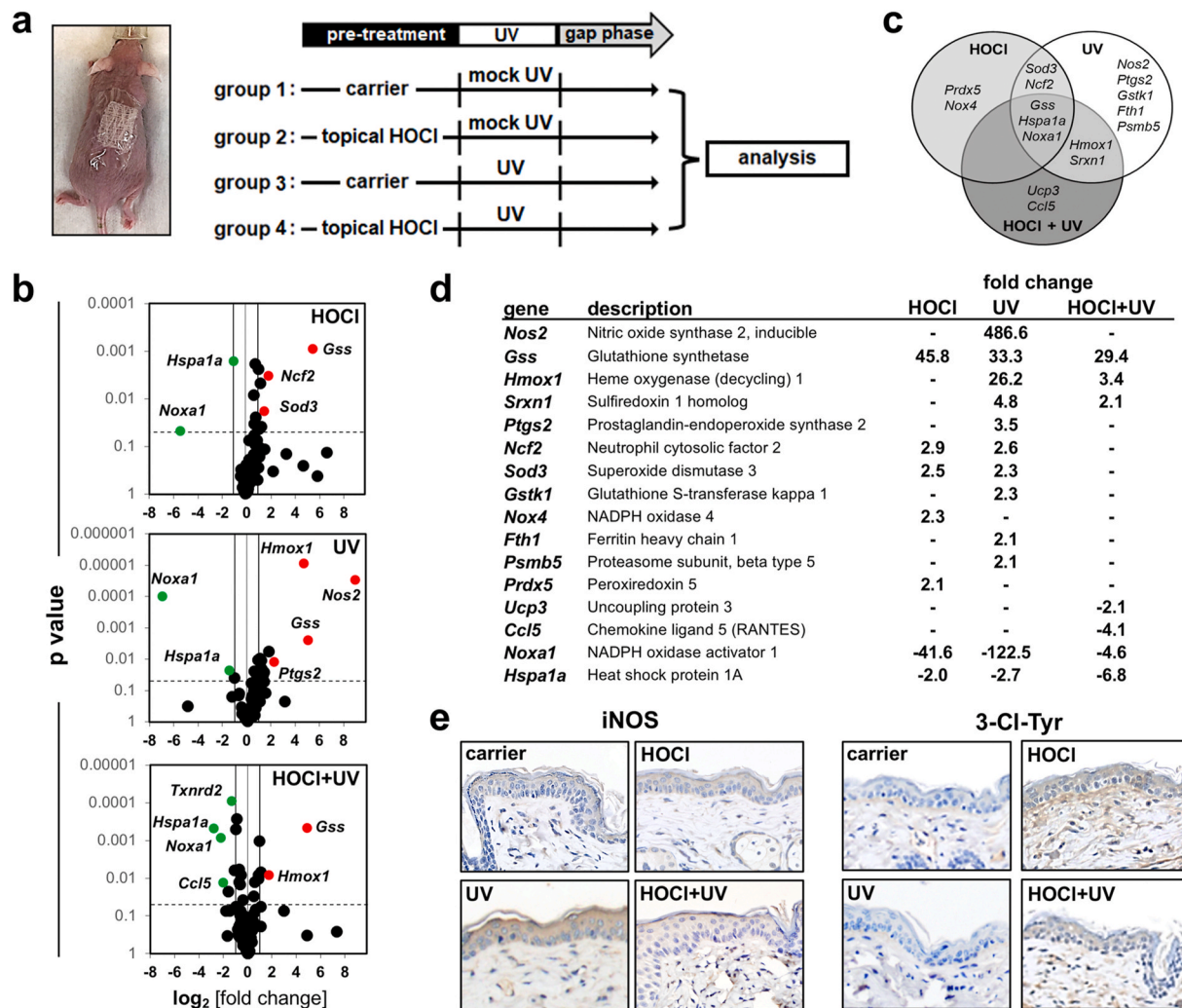


Fig. 2. Short term topical HOCl exposure blocks acute UV-induced inflammatory stress response gene expression in murine skin. (a) Treatment scheme: SKH-1 mice were pretreated ‘with HOCl’ or ‘without HOCl’ (100 μ M, in carrier, 30 min) followed by solar simulated UV exposure (UVA: 9.2 J/cm²; UVB: 480 mJ/cm²); in addition, ‘carrier only’ and ‘UV exposure only’ groups were included (‘groups 1–4’). (b–d) Oxidative Stress Plus RT² Profiler™ PCR Array analysis (6 h after HOCl/UV regimens (‘gap phase’; see scheme in panel a). (b) Differential gene expression (from top to bottom: ‘HOCl only’; ‘UV only’; ‘HOCl + UV’, all versus ‘carrier only control’) as shown by Volcano plot depiction [cut-off lines: expression (fold change) ≥ 2 ; $p < 0.05$; red dots: upregulated; green dots: downregulated]. (c) Venn diagram display (‘HOCl only’ versus ‘UV only’ versus ‘HOCl + UV’; all over carrier control). (d) Tabular summary. (e) Cutaneous IHC analysis examining iNOS expression (left panels) and 3-Cl-Tyr epitopes (groups 1–4; 6 h after HOCl/UV regimens). (For interpretation of the references to colour in this figure legend, the reader is referred to the Web version of this article.)

(‘group 3’; Fig. 2), characterized by pronounced upregulation of inflammatory genes including *Nos2* [encoding inducible nitric oxide synthase 2 (iNOS); 486.6-fold], *Ptgs2* [encoding prostaglandin-endoperoxide synthase 2 (COX-2); 3.5-fold], exclusively sensitive to isolated UV but not HOCl exposure. Moreover, UV-induced modulation of the antioxidant response including upregulation of *Gss* (33.3-fold), *Hmox1* (encoding heme oxygenase 1; 26.2-fold), *Srxn1* (encoding sulfiredoxin 1 homolog; 4.8-fold), *Sod3* (2.3-fold), *Gstk1* (2.3-fold), and *Fth1* (2.1-fold) was detectable.

Next, the effect of HOCl pretreatment on UV-induced inflammatory gene expression (‘group 4’) was explored (Fig. 2). Strikingly, UV-induced upregulation of *Nos2* and *Ptgs2* expression was completely obliterated by cutaneous HOCl pretreatment, an observation supported by immunohistochemical staining for iNOS (Fig. 2e; left panel). In addition, the occurrence of HOCl-induced tissue chlorination stress was substantiated by the detection of 3-chloro-tyrosine-epitopes (Fig. 2e; right panel). A similar attenuation was observable with other stress response genes including *Hmox1*, *Srxn1*, and *Sod3*, but not with *Gss* (that displayed upregulated expression irrespective of HOCl pretreatment).

These differential expression data comparing transcriptional effects of single exposure (HOCl or UV) and combined exposure (HOCl + UV) are summarized by Venn diagram depiction (Fig. 2c). Likewise, the pronounced UV-induced downregulation of *Noxa1* was strongly attenuated upon HOCl pretreatment.

Taken together, these observations indicate that topical HOCl treatment can suppress UV-induced inflammatory and redox stress response gene expression in an acute mouse skin exposure model.

3.3. Topical HOCl exposure blocks inflammatory gene expression elicited by acute UV exposure in AP-1 luciferase reporter SKH-1 mouse skin

Next, the impact of acute HOCl exposure on cutaneous inflammatory signaling was assessed using transgenic SKH-1 reporter mice expressing activator protein 1 (AP-1)-driven luciferase, a powerful genetic tool to monitor UV-induced AP-1 activation and its modulation by topical treatments impacting transcriptional activity of this major pro-inflammatory transcription factor [44,45]. In order to measure the effect of topical HOCl pre-exposure on subsequent solar UV-induced AP-1

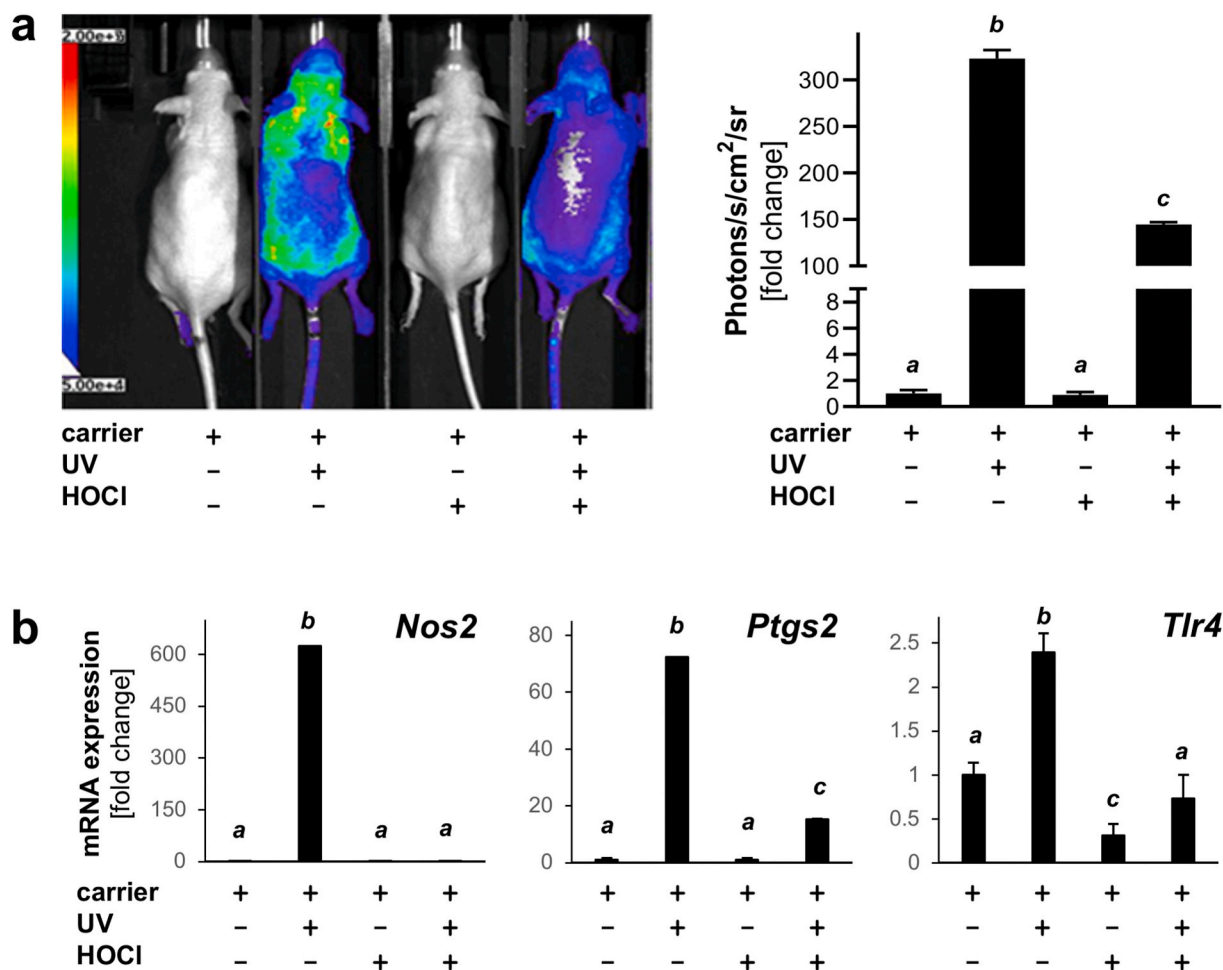


Fig. 3. Topical HOCl blocks UV-induced AP-1 luciferase reporter signaling and inflammatory gene expression in murine skin. (a) AP-1 luciferase reporter SKH-1 mice were pretreated with 'HOCl' (100 μ M) or 'carrier only' followed by solar UV exposure (UVB: 275 mJ/cm²) with inclusion of 'carrier only' and 'UV exposure only' groups; 4 total; n = 3). Mice were injected (24 h after exposure) with luciferin followed by quantitative bioluminescent analysis; bar graph summarizes numerical results. (b) Analysis of UV-induced inflammation-related gene expression (*Nos2*, *Ptgs2*, *Tlr4*) by RT-qPCR (all groups normalized to 'carrier only' group). For all bar graph depictions, quantitative data analysis employed ANOVA with Tukey's post hoc test; means without a common letter differ from each other ($p < 0.05$).

signaling, mouse skin was pretreated 'with HOCl' (100 μ M in carrier) or 'carrier only', followed by 'UV exposure' (UVB: 275 mJ/cm²) or 'mock UV' treatment (Fig. 3). As expected, UV-exposure caused pronounced AP-1 driven luciferase expression as evident from quantitative bioluminescent imaging, characterized by a more than 300-fold upregulation of photon emission over carrier control (Fig. 3a). In contrast, topical HOCl exposure did not induce AP-1 signaling, and, remarkably, HOCl pretreatment strongly attenuated subsequent UV-induced AP-1 activity by more than 50%. Consistent with this observation, UV-induced upregulation of cutaneous inflammatory gene expression (as assessed by single RT-qPCR) was either completely (*Nos2*) or partially down-regulated [*Ptgs2* (4.8-fold), *Tlr4* (encoding toll-like receptor 4; 3.4-fold)].

Taken together, these observations indicate that topical HOCl treatment can suppress AP-1 driven inflammatory gene expression elicited by acute UV exposure as assessed in an engineered murine luciferase reporter system.

3.4. Topical HOCl blocks tumorigenic progression in UV-exposed SKH-1 high risk mouse skin

Next, we explored feasibility of using an HOCl topical regimen (delivered post-UV) for the suppression of cutaneous photocarcinogenesis as examined in an established murine model of UV-

tumorigenesis (UV-exposed SKH-1 'high-risk' mouse skin) (Figs. 4–5). Following a standard exposure regimen of tumorigenic UVB, tumor-prone SKH-1 'high risk' mice were generated by subjecting mice to UV-exposure schedule (112 d duration) followed by a two week gap period, after which topical treatment was initiated, a standard regimen used widely for the identification of chemopreventive therapeutics suppressing photocarcinogenesis [47](Fig. 4a). At the beginning of day 127, 'high risk' mice received either compound in carrier (0.5% HOCl in Vanicream™) or carrier only (Vanicream™; three times per week; over a 24 d period). At the end of the treatment period (d 150), total tumor burden (i.e. tumor volume per mouse) was compared between treatment groups. A significant reduction in average tumor burden was observed in response to HOCl exposure, visible by ocular inspection (Fig. 4b) and substantiated by quantitative analysis (Fig. 4 c,d). In HOCl-treated versus control SKH-1 'high risk' mice, average tumor burden was suppressed by more than 75% [26.2 \pm 19.2 (untreated) versus 6.2 \pm 6.4 (treated)]. Taken together, these data suggest efficacy of topical HOCl to suppress UVB-induced tumorigenesis in a therapeutically relevant post-irradiation treatment regimen.

Next, high risk-skin specimens ['group 1' and 'group 2' (Fig. 4a)] were processed for comparative gene expression profiling and quantitative IHC imaging (Fig. 5). RT² Profiler™ PCR Array analysis revealed that in UV-induced high-risk SKH-1 mouse skin, expression of 20 genes was impacted by HOCl treatment ['group 2' compared to high-risk skin

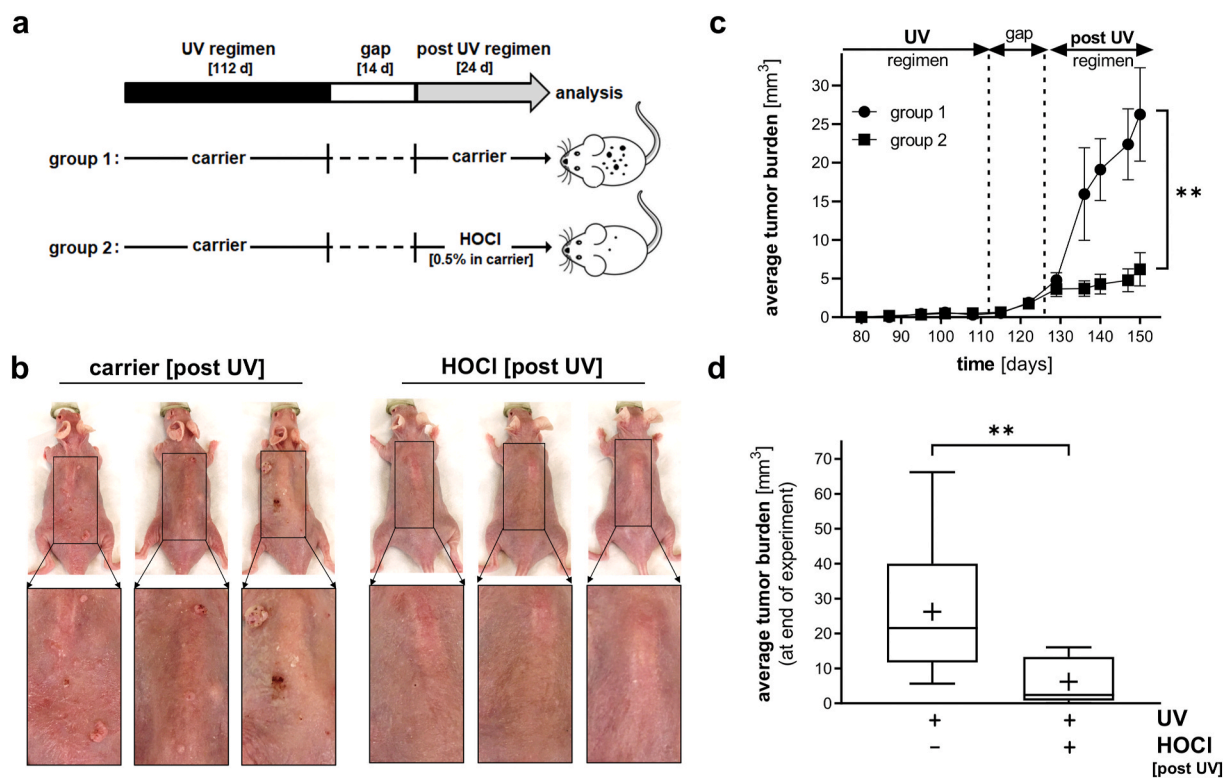


Fig. 4. Topical HOCl blocks tumorigenic progression in UV-induced SKH-1 high-risk mouse skin. (a) Treatment scheme: After implementation of a chronic UVB exposure regimen [up to 190 mJ/cm²; three times per week; 112 d] followed by a gap period (14 d), UV-induced tumor-prone ‘high-risk’ mice were subjected to topical treatment [post UV regimen: ‘carrier only’ (group 1) versus ‘0.5% HOCl in carrier’ (group 2), three times per week, 24 d; n = 10 per group]. (b) At the end of the experiment, dorsal skin was imaged; three representative mice per group are displayed (including 3-fold magnification of rectangular area). (c) Time course of HOCl-induced suppression of average tumor burden [assessed as total tumor volume (mm³) per mouse; p** < 0.01; Mann-Whitney nonparametric statistical analysis]. (d) HOCl-induced suppression of average tumor burden at end of experiment [p** < 0.01 (Mann-Whitney nonparametric statistical analysis); box and whisker plot (minimum to maximum; ‘+’ marks numerical mean)].

treated with carrier only (‘group 1’). Pronounced downregulation of gene expression in response to HOCl was observable impacting inflammatory factors [*Il19* (encoding interleukin 19; 94.3-fold), *Lpo* (encoding lactoperoxidase; 7.3-fold), *Serp1b1* (encoding serine protease inhibitor 1b (7.1-fold), *Ptgs2* (6.2-fold), *Duox1* (encoding dual oxidase 1; 3.1-fold), and *Tr4* (2.9-fold)] (Fig. 5a and b), observations also confirmed by independent single RT-qPCR analysis of selected genes (Fig. 5c). At the same time, modulation of redox regulatory gene expression elicited by HOCl treatment of high-risk skin was observed, including upregulation (≥ 3 -fold): *Fmo2* (encoding flavin containing monooxygenase 2), *Ucp3* (encoding mitochondrial uncoupling protein 3), *Ncf1* (encoding neutrophil cytosol factor 1), *Ncf2* (encoding neutrophil cytosol factor 2), *Cyba* (encoding cytochrome b-245 light chain), *Aox1* (encoding aldehyde oxidase 1), and *Fth1* (encoding ferritin heavy chain 1); downregulation (≥ 3 -fold): *Nqo1* (NAD(P)H dehydrogenase, quinone 1) and *Gpx2* (encoding glutathione peroxidase 2) (Fig. 5a and b). In the context of treatment-induced suppression of skin tumorigenesis, it is also noteworthy that HOCl exposure was associated with upregulated expression of the redox regulatory tumor suppressor gene *Txnip* (encoding thioredoxin interacting protein; up to 4-fold), an observation confirmed by independent single RT-qPCR analysis (Fig. 5b and c) [42].

Consistent with expression data generated at the mRNA level, IHC analysis of tumor tissue originating from high-risk skin (not undergoing HOCl treatment) revealed pronounced staining for IL-19, COX-2, and the proliferation marker Ki67 consistent with expression array analysis (Fig. 5d). Furthermore, comparative IHC analysis of high-risk skin specimens [adjacent to tumor tissue; ‘group 1’ versus ‘group 2’] confirmed significant downregulation of IL-19 and COX-2 protein levels in response to post-UV topical HOCl treatment (Fig. 5e). Likewise, expression of the proliferation marker Ki-67 (observable in the basal

epidermis of high-risk mouse skin) was suppressed by topical HOCl treatment (more than seven-fold), and epidermal thickness, a key characteristic of chronic UV-induced hyperplasia, was diminished by more than 50% in response to HOCl exposure (Fig. 5e). Moreover, the occurrence of tissue chlorination resulting from topical HOCl exposure was substantiated by the detection of 3-chloro-tyrosine-epitopes (Fig. 5e).

Taken together, these data indicate that HOCl treatment can suppress skin photocarcinogenesis as assessed in a murine model of topical post-UV intervention at the phenotypic, transcriptomic, and protein expression levels.

4. Discussion

HOCl is a small molecule electrophile representing an important endogenous microbicidal component of the innate immune system, involved also in inflammatory pathologies and tissue remodeling relevant to wound healing, atherosclerosis, asthma, neurodegeneration, tumorigenesis, and chronological aging [5–9]. Remarkably, HOCl-induced oxidation also represents the mechanistic basis of fresh-water preservation relevant to public drinking water safety and pool disinfection [10–14]. In addition, HOCl consumer products are used on a global scale for surface and skin disinfection targeting viruses, bacteria, and other microbes, a topic of contemporary relevance in the context of the unfolding COVID-19 pandemic [15,22,23].

Here we have investigated for the first time the effects of topical HOCl administration on solar UV-induced skin inflammatory gene expression and carcinogenesis in SKH-1 mouse skin. First, performing array analysis we observed that topical HOCl exposure induces a redox stress response gene expression in human reconstructed epidermis

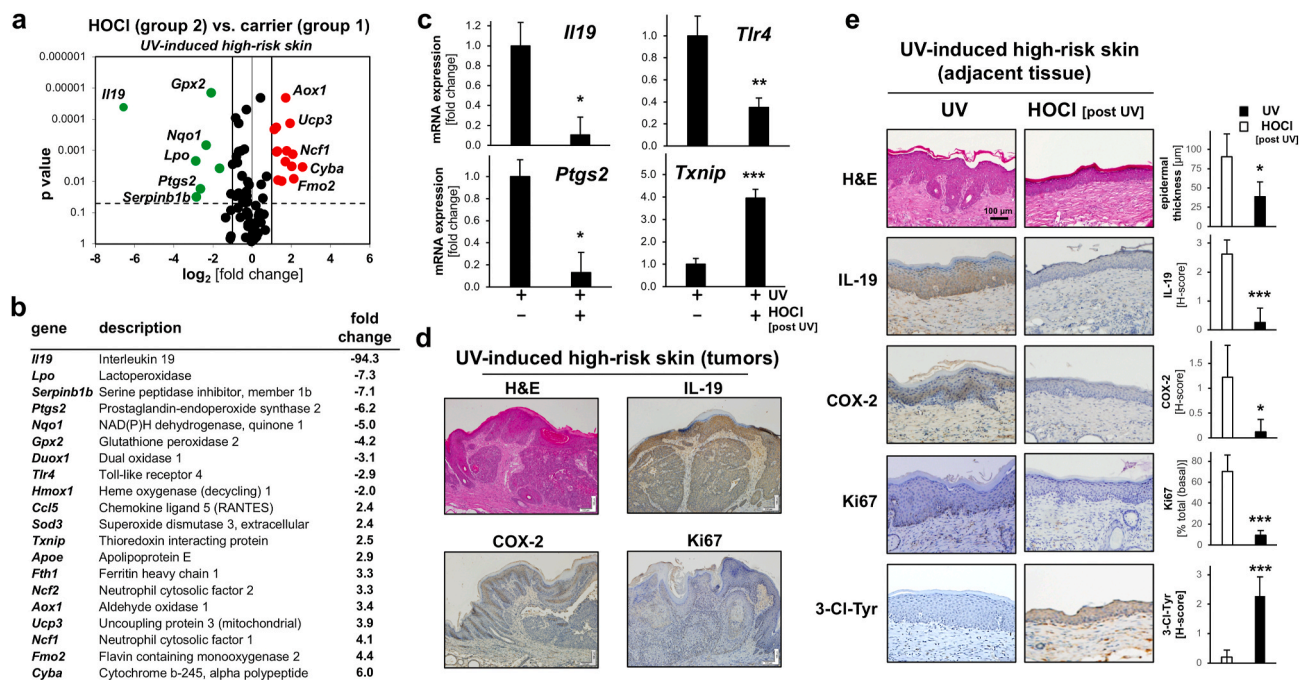


Fig. 5. Topical HOCl modulates inflammatory and redox stress response gene expression in UV-induced SKH-1 high-risk mouse skin. (a) At the end of the murine photocarcinogenesis experiment (as detailed in Fig. 4), dorsal skin was harvested followed by mRNA preparation and Oxidative Stress Plus RT² ProfilerTM PCR Array analysis: Differential gene expression as depicted by volcano plot [UV-induced high-risk skin treated with ‘HOCl in carrier’ (group 2) versus ‘carrier only’ (group 1); cut-off line: expression differential ≥ 2 ; p value ≤ 0.05 ; red dots: upregulated; green dots: downregulated]. (b) Tabular summary of statistically significant expression changes. (c) Single RT-qPCR assessment of gene expression (*Il19*, *Ptgs2*, *Tlr4*, *Txnip*). (d,e) At the end of the experiment, FFPE-skin sections (5 μ m) were analyzed by IHC (H&E, COX-2, IL-19, Ki67) with hematoxylin counterstaining. (d) Tumor cross-sections (‘group 1’ specimens) displaying representative IHC stains; scale bar: 100 μ m. (e) Comparative IHC expression analysis of specimens (group 1 versus group 2; scale bar: 100 μ m) with summary quantification (bar graphs: H-score) including epidermal thickness (μ m), IL-19, COX-2, Ki67, and 3-Cl-Tyr. For bar graphs comparing two groups only, statistical significance was calculated employing the Student’s two-tailed t-test (*p < 0.05; **p < 0.01; ***p < 0.001). (For interpretation of the references to colour in this figure legend, the reader is referred to the Web version of this article.)

(EpiDermTM) (Fig. 1). Second, using SKH-1 mouse skin as a relevant exposure model we observed that topical HOCl induces a redox gene expression profile and that inflammatory gene expression elicited by acute UV exposure was largely suppressed by HOCl pretreatment (Fig. 2). Moreover, the anti-inflammatory cutaneous effects of HOCl pretreatment were substantiated in an established AP-1 luciferase reporter SKH-1 mouse model (Fig. 3). Finally, we were able to demonstrate the chemopreventive efficacy of topical HOCl blocking tumorigenic progression in UV-exposed SKH-1 high risk mouse skin (Figs. 4 and 5).

Obviously, more detailed follow up experiments are needed in order to comprehensively explore HOCl-induced cutaneous effects as a function of various dose regimens, since HOCl modulation of the skin UV-response might differ greatly as a function of exposure time, concentration, pH (carrier and skin), and pre-/co-/post-exposure application [51–53]. For example, rapid HOCl/OCl⁻ photodegradation by solar UVB involving photolytic cleavage (due to absorptivity around 295 nm) has been documented, an effect that is pH dependent, representing a confounding factor circumented in our pilot studies employing an HOCl pre-exposure regimen performed under physiological pH conditions [52, 53].

Importantly, the mechanistic basis underlying HOCl-attenuation of the UV-induced cutaneous redox and inflammatory gene expression response remains to be explored. Hypochlorous acid-induced oxidation of biological targets including proteins, DNA, RNA, and lipids has been documented, and the related oxidation chemistry has been explored in much detail including (i) biochemical mechanisms of formation [such as MPO and related enzymes (TPO/LPO, EPO)], (ii) interaction with other reactive species (such as superoxide radical anion and NO), and (iii) target modification thought to underly microbicidal activity during

neutrophil respiratory burst and inflammation [1–6]. Among HOCl-related posttranslational modifications, chlorination of amino groups (causing chloramine formation), tyrosine chlorination [forming 3-chloro-tyrosine (3-Cl-Tyr)], and oxidation of cysteine residues has been observed in biological specimens contributing to various pathologies including inflammation, metabolic disease, sepsis, neurodegeneration, cancer, and aging [5,6,8,9]. In addition, chlorination-derived protein adducts (including 3-Cl-Tyr) are useful biomarkers of chlorination stress in response to inflammatory dysregulation, caused by either endogenous sources (such as neutrophils) or exogenous exposure (due to environmental or therapeutic HOCl) [54, 55]. Indeed, topical exposure to HOCl as performed in our experiments, either following an acute exposure regimen (Fig. 2) or chronic exposure following solar UV-induced carcinogenesis (Fig. 5), was associated with significant introduction of 3-Cl-Tyr tissue epitopes staining the epidermal and portions of the sub-epidermal layers as detected by IHC analysis, consistent with the occurrence of chlorination stress as a result of the employed exposure regimens. However, molecular identity of specific chlorination targets and their mechanistic role in mediating HOCl-dependent biological effects in skin remains to be explored.

The specific mechanism underlying HOCl modulation of redox and inflammatory gene expression observed by us in human epidermal reconstructions and murine skin remains to be explored. For HOCl-sensitive redox-related genes [including reconstructed human epidermis: *TXNRD2* etc. (Fig. 1); murine skin (acute exposure): *Gss*, *Sod3*, *Prdx5* etc. (Fig. 2); murine skin (‘high risk’): *Nqo1*, *Gpx2*, *Hmox1*, *Sod3* etc. (Fig. 5)] an involvement of the redox-regulatory transcription factor Nrf2 (modulated through HOCl-sensitive cysteine residues of its negative regulator Keap1) seems likely, a hypothesis to be substantiated by further experiments [56,57].

Previous clinical research has demonstrated that HOCl-dependent cysteine oxidation causes IKK (I κ B kinase) inactivation (through post-translational modification of Cys114 and 115) resulting in I κ B stabilization and subsequent inhibition of NF κ B nuclear translocation with suppression of inflammatory gene expression impacting established molecular mediators including the enzymes iNOS and COX-2 [8,9]. Indeed, cumulative evidence suggests that IKK inactivation represents the crucial mechanistic basis underlying HOCl-dependent therapeutic efficacy targeting psoriasis, a mechanism that has also been substantiated suppressing melanoma progression as a result of myeloid cell-derived HOCl [8,9]. Also, when examined in a mouse model of NF κ B-driven acute radiation dermatitis, it has been reported that topical HOCl inhibited NF κ B-dependent gene expression, decreased disease severity, and prevented skin ulceration. These specific IKK-directed effects might also underly the documented clinical efficacy of topical HOCl in the treatment of other inflammatory skin conditions including atopic dermatitis, pruritus, seborrheic dermatitis, acne vulgaris, diabetic ulcers, wound healing, and scar prevention [24,25]. Remarkably, a similar mechanism might be involved in HOCl antagonism of solar UV-induced AP-1 activation observed by us for the first time using a transgenic reporter mouse (Fig. 3). Indeed, the transcription factor AP-1, crucially involved in skin inflammatory dysregulation and photocarcinogenesis, has been shown to be sensitive to electrophile-dependent cysteine adduction (c-Fos: Cys154; c-Jun: Cys272) suppressing skin photocarcinogenesis, a hypothesis to be tested by future experiments [44]. However, the specific mechanistic involvement of NF κ B and AP-1 in the HOCl-induced attenuation of UV-induced skin inflammatory gene expression and carcinogenesis remains to be elucidated. Certainly, downregulation of major inflammatory mediators, including *Nos2* and *Ptgs2* might be attributable to HOCl-dependent antagonism targeting these two major pro-inflammatory regulators known to synergize regulating inflammatory gene expression, a scenario to be explored in more adequate detail [58,59].

It is also remarkable that in high-risk mouse skin, the inflammatory cytokine IL-19 displayed the most pronounced downregulation (at the mRNA and protein levels) in response to HOCl treatment (Fig. 5). IL-19 has now been identified as a crucial pathological driver in psoriasis, atopic dermatitis, and cutaneous T cell lymphoma in human patients suggesting that downregulation of IL-19 could be mechanistically involved in HOCl-dependent suppression of tumorigenesis [60–64]. Indeed, STAT3, the transcription factor mediating JAK/STAT signaling downstream of IL-19-dependent activation of the IL-20R1/IL-20R2 receptor heterodimer is an established tumorigenic factor in UV-induced squamous cell carcinoma [65]. Thus, HOCl-modulation of IL-19 (demonstrated here for the first time) might open up novel therapeutic avenues for cutaneous anti-inflammatory intervention.

HOCl adduction of relevant molecular targets remains poorly understood, and apart from modulation of inflammatory pathways HOCl has also been shown to display cancer cell-directed activities including GRP78-mediated modulation of ER stress, autophagy, and proteotoxicity. Specifically, GRP78-directed Lys353 oxidation and other molecular pathways have been involved in HOCl-associated antitumorogenic activity, a topic to be explored by future experiments in the context of HOCl-suppression of photocarcinogenesis [9,66,67]. Additionally, upregulation of the tumor suppressor gene *Txnip* observed by us in response to HOCl-exposure in the context of our UV-induced SKH-1 high risk mouse model might also be involved in the anti-tumorogenic activity of topical HOCl (Fig. 5b and c).

Taken together, these data illuminate for the first time the molecular consequences of HOCl-exposure in relevant cutaneous organotypic and murine models assessing inflammatory gene expression and modulation of UV-induced carcinogenesis. These observations if translatable to human skin provide novel insights on molecular consequences of chlorination stress relevant to environmental exposure and therapeutic intervention.

Declaration of competing interest

The authors declare that they have no known competing financial interests or personal relationships that could have appeared to influence the work reported in this paper.

Acknowledgements

Supported in part by grants from the National Institutes of Health (1R01CA229418, 1R03CA230949, 1R21ES029579, 1P01CA229112, ES007091, ES006694, and UA Cancer Center Support Grant CA023074). The content is solely the responsibility of the authors and does not necessarily represent the official views of the National Cancer Institute or the National Institutes of Health.

References

- [1] J.M. Albrich, C.A. McCarthy, J.K. Hurst, Biological reactivity of hypochlorous acid: implications for microbicidal mechanisms of leukocyte myeloperoxidase, *Proc. Natl. Acad. Sci. U. S. A.* 78 (1981) 210–214.
- [2] C.L. Hawkins, M.J. Davies, Hypochlorite-induced damage to DNA, RNA, and polynucleotides: formation of chloramines and nitrogen-centered radicals, *Chem. Res. Toxicol.* 15 (2002) 83–92.
- [3] C.L. Hawkins, D.I. Pattison, M.J. Davies, Hypochlorite-induced oxidation of amino acids, peptides and proteins, *Amino Acids* 25 (2003) 259–274.
- [4] D.I. Pattison, C.L. Hawkins, M.J. Davies, Hypochlorous acid-mediated protein oxidation: how important are chloramine transfer reactions and protein tertiary structure? *Biochemistry* 46 (2007) 9853–9864.
- [5] G. Bauer, HOCl and the control of oncogenesis, *J. Inorg. Biochem.* 179 (2018) 10–23.
- [6] A. Ulfig, L.I. Leichert, The effects of neutrophil-generated hypochlorous acid and other hypohalous acids on host and pathogens, *Cell. Mol. Life Sci.* 78 (2021) 385–414.
- [7] M. Casciaro, E. Di Salvo, E. Pace, E. Ventura-Spagnolo, M. Navarra, S. Gangemi, Chlorinative stress in age-related diseases: a literature review, *Immun. Ageing* 14 (2017) 21.
- [8] T.H. Leung, L.F. Zhang, J. Wang, S. Ning, S.J. Knox, S.K. Kim, Topical hypochlorite ameliorates NF- κ B-mediated skin diseases in mice, *J. Clin. Invest.* 123 (2013) 5361–5370.
- [9] T.W. Liu, S.T. Gammon, P. Yang, D. Fuentes, D. Piwnicka-Worms, Myeloid cell-derived HOCl is a paracrine effector that trans-inhibits IKK/NF- κ B in melanoma cells and limits early tumor progression, *Sci. Signal.* 14 (677) (2021), eaax5971.
- [10] World Health Organization, Guidelines for Safe Recreational Water Environments: VOLUME 2 SWIMMING POOLS and SIMILAR ENVIRONMENTS, 2006, ISBN 92 4 154680 8.
- [11] T. H. I. C. P. A. C. (HICPAC), Guideline for Disinfection and Sterilization in Healthcare Facilities, Centers for Disease Control and prevention (CDC), 2008.
- [12] S.D. Richardson, D.M. DeMarini, M. Kogevinas, P. Fernandez, E. Marco, C. Lourencetti, C. Balleste, D. Heederik, K. Meliefste, A.B. McKague, R. Marcos, L. Font-Ribera, J.O. Grimalt, C.M. Villanueva, What's in the pool? A comprehensive identification of disinfection by-products and assessment of mutagenicity of chlorinated and brominated swimming pool water, *Environ. Health Perspect.* 118 (2010) 1523–1530.
- [13] E.I. Prest, F. Hammes, M.C. van Loosdrecht, J.S. Vrouwenvelder, Biological stability of drinking water: controlling factors, methods, and challenges, *Front. Microbiol.* 7 (2016) 45.
- [14] US Environmental Protection Agency (EPA) Ground water and drinking water. <https://www.epa.gov/ground-water-and-drinking-water/emergency-disinfection-drinking-water> (accessed: 4-29-2021).
- [15] EPA (US Environmental Protection Agency); List N. Disinfectants for Use against SARS-CoV-2.
- [16] A. Pardo, K. Nevo, D. Vigiser, A. Lazarov, The effect of physical and chemical properties of swimming pool water and its close environment on the development of contact dermatitis in hydrotherapists, *Am. J. Ind. Med.* 50 (2007) 122–126.
- [17] I. Helenius, T. Haahtela, Allergy and asthma in elite summer sport athletes, *J. Allergy Clin. Immunol.* 106 (2000) 444–452.
- [18] Y. Schoefer, A. Zutavern, I. Brockow, T. Schafer, U. Kramer, B. Schaff, O. Herbarth, A. von Berg, H.E. Wichmann, J. Heinrich, L.s. group, Health risks of early swimming pool attendance, *Int. J. Hyg. Environ. Health* 211 (2008) 367–373.
- [19] L. Font-Ribera, M. Kogevinas, J.P. Zock, M.J. Nieuwenhuijsen, D. Heederik, C. M. Villanueva, Swimming pool attendance and risk of asthma and allergic symptoms in children, *Eur. Respir. J.* 34 (2009) 1304–1310.
- [20] A. Goma, R. de Lluís, J. Roca-Ferrer, J. Lafuente, C. Picado, Respiratory, ocular and skin health in recreational and competitive swimmers: beneficial effect of a new method to reduce chlorine oxidant derivatives, *Environ. Res.* 152 (2017) 315–321.
- [21] M.S. Block, B.G. Rowan, Hypochlorous acid: a review, *J. Oral Maxillofac. Surg.* 78 (2020) 1461–1466.
- [22] G. Kampf, D. Todt, S. Pfaender, E. Steinmann, Persistence of coronaviruses on inanimate surfaces and their inactivation with biocidal agents, *J. Hosp. Infect.* 104 (2020) 246–251.

- [23] N. Giarratana, B. Rajan, K. Kamala, M. Mendenhall, G. Reiner, A sprayable Acid-Oxidizing solution containing hypochlorous acid (AOS2020) efficiently and safely inactivates SARS-Cov-2: a new potential solution for upper respiratory tract hygiene, Feb11, Eur. Arch. Oto-Rhino-Laryngol. (2021) 1–5 ([Epub ahead of print]).
- [24] T. Fukuyama, B.C. Martel, K.E. Linder, S. Ehling, J.R. Ganchingco, W. Baumer, Hypochlorous acid is antipruritic and anti-inflammatory in a mouse model of atopic dermatitis, Clin. Exp. Allergy 48 (2018) 78–88.
- [25] J.Q. Del Rosso, N. Bhatia, Status report on topical hypochlorous acid: clinical relevance of specific formulations, potential modes of action, and study outcomes, J Clin Aesthet Dermatol 11 (2018) 36–39.
- [26] J. Cadet, T. Douki, Formation of UV-induced DNA damage contributing to skin cancer development, Photochem. Photobiol. Sci. 17 (2018) 1816–1841.
- [27] G.T. Wondrak, Let the sun shine in: mechanisms and potential for therapeutics in skin photodamage, Curr. Opin. Invest. Drugs 8 (2007) 390–400.
- [28] G.T. Wondrak, in: L.M. Alberts DaH (Ed.), Sunscreen-Based Skin Protection against Solar Insult: Molecular Mechanisms and Opportunities. Fundamentals of Cancer Prevention, Springer Science & Business Media, 2019, pp. 377–404.
- [29] Y. Wang, D. Gao, D.P. Atencio, E. Perez, R. Saladi, J. Moore, D. Guevara, B. S. Rosenstein, M. Lebwohl, H. Wei, Combined subcarcinogenic benzo[a]pyrene and UVA synergistically caused high tumor incidence and mutations in H-ras gene, but not p53, in SKH-1 hairless mouse skin, Int. J. Canc. 116 (2005) 193–199.
- [30] P. Boffetta, F. Nyberg, Contribution of environmental factors to cancer risk, Br. Med. Bull. 68 (2003) 71–94.
- [31] S. Nair, V.D. Kekatpure, B.L. Judson, A.B. Rifkind, R.D. Granstein, J.O. Boyle, K. Subbaramaiah, J.B. Guttenplan, A.J. Dannenberg, UVR exposure sensitizes keratinocytes to DNA adduct formation, Canc. Prev. Res. 2 (2009) 895–902.
- [32] C.B. Klein, J. Leszczynska, C. Hickey, T.G. Rossman, Further evidence against a direct genotoxic mode of action for arsenic-induced cancer, Toxicol. Appl. Pharmacol. 222 (2007) 289–297.
- [33] R. Saladi, L. Austin, D. Gao, Y. Lu, R. Phelps, M. Lebwohl, H. Wei, The combination of benzo[a]pyrene and ultraviolet A causes an in vivo time-related accumulation of DNA damage in mouse skin, Photochem. Photobiol. 77 (2003) 413–419.
- [34] C. Baudouin, M. Charveron, R. Tarroux, Y. Gall, Environmental pollutants and skin cancer, Cell Biol. Toxicol. 18 (2002) 341–348.
- [35] R.B. Cope, K. Imsilp, C.K. Morrow, J. Hartman, D.J. Schaeffer, L.G. Hansen, Exposure to soil contaminated with an environmental PCB/PCDD/PCDF mixture modulates ultraviolet radiation-induced non-melanoma skin carcinogenesis in the CrI:SKH1-hrBR hairless mouse, Canc. Lett. 191 (2003) 145–154.
- [36] J. Perer, J. Jandova, J. Fimbres, E.Q. Jennings, J.J. Galligan, A. Hua, G. T. Wondrak, The sunless tanning agent dihydroxyacetone induces stress response gene expression and signaling in cultured human keratinocytes and reconstructed epidermis, Redox Biol 36 (2020) 101594.
- [37] R. Justiniano, L. de Faria Lopes, J. Perer, A. Hua, S.L. Park, J. Jandova, M. S. Baptista, G.T. Wondrak, The endogenous tryptophan-derived photoproduct 6-formylindolo[3,2-b]carbazole (FICZ) is a nanomolar photosensitizer that can be harnessed for the photodynamic elimination of skin cancer cells in vitro and in vivo, Photochem. Photobiol. 97 (2021) 180–191.
- [38] S.L. Park, R. Justiniano, J.D. Williams, C.M. Cabello, S. Qiao, G.T. Wondrak, The tryptophan-derived endogenous aryl hydrocarbon receptor ligand 6-Formylindolo [3,2-b]Carbazole is a nanomolar UVA photosensitizer in epidermal keratinocytes, J. Invest. Dermatol. 135 (2015) 1649–1658.
- [39] S.D. Lamore, G.T. Wondrak, Zinc pyrithione impairs zinc homeostasis and upregulates stress response gene expression in reconstructed human epidermis, Biometals 24 (2011) 875–890.
- [40] S. Tao, R. Justiniano, D.D. Zhang, G.T. Wondrak, The Nrf2-inducers tanshinone I and dihydrotanshinone protect human skin cells and reconstructed human skin against solar simulated UV, Redox Biol 1 (2013) 532–541.
- [41] J. Jandova, J. Perer, A. Hua, J.A. Snell, G.T. Wondrak, Genetic target modulation employing CRISPR/Cas9 identifies glyoxalase 1 as a novel molecular determinant of invasion and metastasis in A375 human malignant melanoma cells in vitro and in vivo, Cancers 12 (6) (2020) 1369.
- [42] J. Jandova, G.T. Wondrak, Genomic GLO1 deletion modulates TXNIP expression, glucose metabolism, and redox homeostasis while accelerating human A375 malignant melanoma tumor growth, Redox Biol 39 (2021) 101838.
- [43] M. Rojo de la Vega, D.D. Zhang, G.T. Wondrak, Topical bixin confers NRF2-dependent protection against photodamage and hair graying in mouse skin, Front. Pharmacol. 9 (2018) 287.
- [44] S.E. Dickinson, T.F. Melton, E.R. Olson, J. Zhang, K. Saboda, G.T. Bowden, Inhibition of activator protein-1 by sulforaphane involves interaction with cysteine in the cFos DNA-binding domain: implications for chemoprevention of UVB-induced skin cancer, Canc. Res. 69 (2009) 7103–7110.
- [45] K. Blohm-Mangone, N.B. Burkett, S. Tahsin, P.B. Myrdal, A. Aodah, B. Ho, J. Janda, M. McComas, K. Saboda, D.J. Roe, Z. Dong, A.M. Bode, E.F. Petricoin 3rd, V. S. Calvert, C. Curiel-Lewandrowski, D.S. Alberts, G.T. Wondrak, S.E. Dickinson, Pharmacological TLR4 antagonism using topical resatorvid blocks solar UV-induced skin tumorigenesis in SKH-1 mice, Canc. Prev. Res. 11 (2018) 265–278.
- [46] Y.P. Lu, Y.R. Lou, J.G. Xie, Q. Peng, W.J. Shih, Y. Lin, A.H. Conney, Tumorigenic effect of some commonly used moisturizing creams when applied topically to UVB-pretreated high-risk mice, J. Invest. Dermatol. 129 (2009) 468–475.
- [47] R. Justiniano, J. Perer, A. Hua, M. Fazel, A. Krajcsnik, C.M. Cabello, G.T. Wondrak, A topical zinc ionophore blocks tumorigenic progression in UV-exposed SKH-1 high-risk mouse skin, Photochem. Photobiol. 93 (2017) 1472–1482.
- [48] S. Grehan, C. Allan, E. Tse, D. Walker, J.M. Taylor, Expression of the apolipoprotein E gene in the skin is controlled by a unique downstream enhancer, J. Invest. Dermatol. 116 (2001) 77–84.
- [49] M. Conrad, C. Jakupoglu, S.G. Moreno, S. Lippl, A. Banjac, M. Schneider, H. Beck, A.K. Hatzopoulos, U. Just, F. Sinowatz, W. Schmahl, K.R. Chien, W. Wurst, G. W. Bornkamm, M. Brielmeier, Essential role for mitochondrial thioredoxin reductase in hematopoiesis, heart development, and heart function, Mol. Cell Biol. 24 (2004) 9414–9423.
- [50] M. Canavese, F. Altruda, L. Silengo, Therapeutic efficacy and immunological response of CCL5 antagonists in models of contact skin reaction, PLoS One 5 (2010), e8725.
- [51] N. Kishimoto, H. Nishimura, Effect of pH and molar ratio of pollutant to oxidant on a photochemical advanced oxidation process using hypochlorite, Environ. Technol. 36 (2015) 2436–2442.
- [52] L.H. Nowell, J. Hoigne, Photolysis and of aqueous chlorine at sunlight ultraviolet wavelengths -I. Degradation rates, Water Res. 26 (1992) 593–598.
- [53] M.J. Watts, K.G. Linden, Chlorine photolysis and subsequent OH radical production during UV treatment of chlorinated water, Water Res. 41 (2007) 2871–2878.
- [54] S.L. Hazen, J.W. Heinecke, 3-Chlorotyrosine, a specific marker of myeloperoxidase-catalyzed oxidation, is markedly elevated in low density lipoprotein isolated from human atherosclerotic intima, J. Clin. Invest. 99 (1997) 2075–2081.
- [55] J.I. Kang Jr., J.W. Neidigh, Hypochlorous acid damages histone proteins forming 3-chlorotyrosine and 3,5-dichlorotyrosine, Chem. Res. Toxicol. 21 (2008) 1028–1038.
- [56] J. Pi, Q. Zhang, C.G. Woods, V. Wong, S. Collins, M.E. Andersen, Activation of Nrf2-mediated oxidative stress response in macrophages by hypochlorous acid, Toxicol. Appl. Pharmacol. 226 (2008) 236–243.
- [57] N. Kavian, S. Mehral, M. Jeljeli, N.E.B. Saidu, C. Nicco, O. Cerles, S. Chouzenoux, A. Cauvet, C. Camus, M. Ait-Djoudi, C. Chereau, S. Keridine-Romer, Y. Allanore, F. Bateau, The nrf2-antioxidant response element signaling pathway controls fibrosis and autoimmunity in scleroderma, Front. Immunol. 9 (2018) 1896.
- [58] A. Dhar, M.R. Young, N.H. Colburn, The role of AP-1, NF-kappaB and ROS/NOS in skin carcinogenesis: the JB6 model is predictive, Mol. Cell. Biochem. 234–235 (2002) 185–193.
- [59] S.H. Kim, J.M. Oh, J.H. No, Y.J. Bang, Y.S. Juhn, Y.S. Song, Involvement of NF-kappaB and AP-1 in COX-2 upregulation by human papillomavirus 16 E5 oncoprotein, Carcinogenesis 30 (2009) 753–757.
- [60] C.H. Hsing, H.H. Li, Y.H. Hsu, C.L. Ho, S.S. Chuang, K.M. Lan, M.S. Chang, The distribution of interleukin-19 in healthy and neoplastic tissue, Cytokine 44 (2008) 221–228.
- [61] C.H. Hsing, H.C. Cheng, Y.H. Hsu, C.H. Chan, C.H. Yeh, C.F. Li, M.S. Chang, Upregulated IL-19 in breast cancer promotes tumor progression and affects clinical outcome, Clin. Canc. Res. 18 (2012) 713–725.
- [62] E. Witte, G. Kokolakis, K. Witte, S. Philipp, W.D. Doecke, N. Babel, B.M. Wittig, K. Warszawska, A. Kurek, M. Erdmann-Keding, S. Kunz, K. Asadullah, M.E. Kadin, H.D. Volk, W. Sterry, K. Wolk, R. Sabat, IL-19 is a component of the pathogenetic IL-23/IL-17 cascade in psoriasis, J. Invest. Dermatol. 134 (2014) 2757–2767.
- [63] T. Oka, M. Sugaya, N. Takahashi, R. Nakajima, S. Otobe, M. Kabasawa, H. Suga, T. Miyagaki, Y. Asano, S. Sato, Increased interleukin-19 expression in cutaneous T-cell lymphoma and atopic dermatitis, Acta Derm. Venereol. 97 (2017) 1172–1177.
- [64] R.J. Konrad, R.E. Higgs, G.H. Rodgers, W. Ming, Y.W. Qian, N. Bivi, J.K. Mack, R. W. Siegel, B.J. Nickoloff, Assessment and clinical relevance of serum IL-19 levels in psoriasis and atopic dermatitis using a sensitive and specific novel immunoassay, Sci. Rep. 9 (2019) 5211.
- [65] E. Macias, D. Rao, J. Digiovanni, Role of stat3 in skin carcinogenesis: insights gained from relevant mouse models, J Skin Cancer (2013) 684050, 2013.
- [66] J. Ning, Z. Lin, X. Zhao, B. Zhao, J. Miao, Inhibiting lysine 353 oxidation of GRP78 by a hypochlorous probe targeting endoplasmic reticulum promotes autophagy in cancer cells, Cell Death Dis. 10 (2019) 858.
- [67] E. Freund, L. Miebach, M.B. Stope, S. Bekeschus, Hypochlorous acid selectively promotes toxicity and the expression of danger signals in human abdominal cancer cells, Oncol. Rep. 45 (5) (2021) 71.